ELSEVIER

Journal of Fluids and Structures 25 (2009) 751–765

JOURNAL OF FLUIDS AND STRUCTURES

www.elsevier.com/locate/jfs

Nonlinear analysis of orbital motion of a rotor subject to leakage air flow through an interlocking seal

W.Z. Wang[a], Y.Z. Liu[a,*], G. Meng[b], P.N. Jiang[c]

[a]*Key Lab of Education Ministry for Power Machinery and Engineering, Shanghai Jiao Tong University, 800 Dongchuan Road, Shanghai 200240, China*

[b]*State Key Lab of Mechanical System and Vibration, Shanghai Jiao Tong University, 800 Dongchuan Road, Shanghai 200240, China*

[c]*Department of R&D, Shanghai Turbine Company, 333 Jiang Chuan Road, Shanghai 200240, China*

Received 30 November 2007; accepted 10 July 2008
Available online 10 May 2009

Abstract

A nonlinear mathematical model for orbital motion of the rotor under the influence of leakage flow through a labyrinth seal was established in the present study. An interlocking seal was chosen for study. The rotor–seal system was modeled as a Jeffcot rotor subject to aerodynamic forcing induced by the leakage flow. Particular attention was placed on the serpentine flow path by spatially separating the aerodynamic force on the rotor surface into two parts, e.g., the seal clearance and the cavity volume. Spatio-temporal variation of the aerodynamic force on the rotor surface in the coverage of the seal clearance and the cavity volume was delineated by using the Muzynska model and perturbation analysis, respectively. The governing equation of rotor dynamics, which was incorporated with the aerodynamic force integrated over all seal clearances and cavity volumes, was solved by using the fourth-order Runge–Kutta method to obtain the orbit of the whirling rotor. Stability of the rotating rotor was inspected using the Liapunov first method. The results convincingly demonstrate that the destabilization speed of the rotor was reduced due to the aerodynamic force induced by the leakage flow through the interlocking seal. The nonlinear analysis method proposed in the present study is readily applied to dynamics of various rotor–seal systems with labyrinth seals.

Keywords: Nonlinear analysis; Orbital motion; Labyrinth seal; Muzynska model; Perturbation analysis

1. Introduction

Labyrinth seals in which a series of teeth are periodically placed on the rotor or/and stator walls are widely employed in turbo machines to suppress leakage flow through the narrow radial gap between the rotor and the stator. The serpentine geometry of the highly dissipative flow path complicates the three-dimensional leakage flow, which is closely coupled with the rotating and whirling rotor. The rotor which is subject to a strong aerodynamic force induced by the leakage flow through the labyrinth seals may exhibit nonlinear behavior in its orbital motion, resulting in complex rotor dynamics. Accordingly, a quantitative understanding of the influence of the leakage flow on the orbital motion of the rotor is of essential significance.

*Corresponding author. Tel./fax: +86 21 34206582.
E-mail address: yzliu@sjtu.edu.cn (Y.Z. Liu).

0889-9746/$ - see front matter © 2009 Elsevier Ltd. All rights reserved.
doi:10.1016/j.jfluidstructs.2008.07.009

Nomenclature

A_n	unsteady cross-sectional area of the cavity (m^2)
A_0	steady annular flow area (m^2)
B	tooth height (m)
C_0	orifice contraction coefficient
C_1	kinetic energy carry-over coefficient
C_r	steady radial clearance (m)
Dh_0	steady hydraulic diameter of the cross-sectional area of the cavity (m)
Dh	unsteady hydraulic diameter of the cross-sectional area of the cavity (m)
D_e	damping coefficient of the rotor (N s/m)
D_i	equivalent damping of air flow at the ith seal clearance (N s/m)
D_{br}	equivalent damping of oil film in the journal bearings (N s/m)
e	displacement of the rotor from the central position (m/s)
$F(t)\|_{ca}$	total air reaction force in the cavities (N)
$F_x(t)\|_{br}$	journal bearing reaction force component in the X direction (N)
$F_y(t)\|_{br}$	journal bearing reaction force component in the Y direction (N)
$F_x(t)\|_{ca}$	cavity reaction force component in the X direction (N)
$F_y(t)\|_{ca}$	cavity reaction force component in the Y direction (N)
$F_x(t)\|_{cl}$	seal clearance reaction force component in the X direction (N)
$F_y(t)\|_{cl}$	seal clearance reaction force component in the Y direction (N)
g_0	empirical coefficient determined by the structure of the labyrinth seal
H	unsteady labyrinth seal radial clearance (m)
$H_1(t,\theta)$	perturbation clearance (m)
K_e	stiffness of the rotor (N/m)
K_t	equivalent stiffness of air flow at the ith seal clearance (N/m)
K_{br}	equivalent stiffness of oil film in the journal bearings (N/m)
L	pitch of the cavity (m)
m_0	leakage flow through the labyrinth seal (kg/s)
m_r	mass of the rotor (kg)
m_{fl}	equivalent mass of air flow at the ith seal clearance (kg)
m_{for}	equivalent mass of oil film in the journal bearings (kg)
N	tooth number
n_0	empirical coefficient determined by the structure of the labyrinth seal
n	pressure ratio of the labyrinth seal
P_{cli}	steady pressure at the ith seal clearance (Pa)
P_{0i}	steady pressure at the ith cavity (Pa)
P_i	unsteady pressure at the ith cavity (Pa)
$P_{1i}(t,\theta)$	perturbation pressure in the ith cavity (Pa)
$\dot{q}_{0i}$	steady leakage rate per unit length (kg/s m)
$\dot{q}_i$	unsteady leakage rate per unit length (kg/s m)
$\dot{q}_{1i}(t,\theta)$	perturbation leakage flow rate per unit length (kg/s m)
R	gas constant (J/kg K)
R_s	rotor radius (m)
R_a	Reynolds number of the axial flow
R_v	Reynolds number of circumferential flow
t_{cl}	time of air flow through the seal clearance (s)
T	temperature in the labyrinth seal (K)
V_{acli}	steady axial veclity at the ith seal clearance (m/s)
V_{0i}	steady circumferential velocities at the ith cavity (m/s)
V_i	unsteady circumferential velocities at the ith cavity (m/s)
$V_{1i}(t,\theta)$	perturbation pressure at the ith cavity (m/s)
W	width of tooth (m)
$(x_{o'}(t), y_{o'}(t))$	x and y coordinates of the whirling rotor (m)
z	inlet loss coefficient of the labyrinth seal

Greek symbols

α_r	dimensionless shear stress length at the rotor wall
α_s	dimensionless shear stress length at the stator wall
γ	specific heat ratio
ε	eccentricity ratio
η	imaginary number
θ	azimuthal position
λ	friction coefficient
ν	kinematic viscosity (m^2/s)
ρ_{0i}	steady gas density in the ith cavity (kg/m^3)
ρ_i	unsteady gas density in the ith cavity (kg/m^3)
σ	gradient coefficient of loss of friction
τ_{br}	ratio of circumferential velocity of the oil film in the journal bearings to the rotor surface speed
τ_i	ratio of circumferential velocity of the air flow at the ith seal clearance to the rotor surface speed

τ_{ri}	unsteady shear stresses at the rotor wall (N/m^2)	$\tau_{s1i}(t,\theta)$	perturbation shear stresses at the stator wall (N/m^2)
τ_{r0i}	steady shear stresses at the rotor wall (N/m^2)	ω	rotating speed of the rotor (rpm)
$\tau_{r1i}(t,\theta)$	perturbation shear stresses at the rotor wall (N/m^2)	*Subscripts*	
τ_{si}	unsteady shear stresses at the stator wall (N/m^2)	*cl*	clearance of the labyrinth seal
		ca	cavity volume of the labyrinth seal
τ_{s0i}	steady shear stresses at the stator wall (N/m^2)	*br*	journal bearing

Considerable numerical efforts have been made to understand the influence of the leakage flow through labyrinth seals on rotor dynamics. Among others, a linearized force–displacement model of rotor dynamics associated with leakage flow through seals was developed by Kostyuk (1972) and Iwatsubo (1980), yielding a school of coefficients characterizing the aerodynamic force on the rotor. Spatio-temporal variation of the pressure and shear force on the rotor surface (Childs and Scharrer, 1986), which is caused by deviation of the rotor from the central position, was extensively taken into account in the linear model. Subsequently, the rotor dynamics coefficients associated with the leakage air flow through various labyrinth seals were numerically calculated, e.g., the straight-through seal (Childs and Scharrer, 1987; Rosen, 1986; Dursun and Kazakia, 1995; Yucel and Kazakia, 2001), the stepped seal (Dursun, 2002; Yucel, 2004) and the honeycomb seal (Kleynhans, 1996). Furthermore, numerical calculations of unsteady static pressure in cavities of the interlocking seal by employing perturbation analysis (Dursun and Kazakia, 1995; Childs and Scharrer, 1987; Dursun, 2002; Yucel, 2004) were demonstrated to be in favorable agreement with experimental results by Liu et al. (2007). Recently, the authors presented a linear model of calculating rotor dynamics coefficients, which are related to leakage steam flow through labyrinth seals; particular attention was placed on incorporating thermal properties of the steam fluid into the derivation of rotor dynamics coefficients. However, the above-mentioned linear model was reduced on the basis of a preconditioned track of the whirling rotor, which slightly deviates from the statically balanced position; otherwise, large deviation of the whirling rotor in reference to the clearance size would result in nonlinear motion behavior of the aerodynamically forced rotor, e.g., lock-on frequency and kick amplitude, which could not be accurately predicted by the linearized force–displacement model (Dursun and Kazakia, 1995; Kleynhans, 1996; Dursun, 2002; Yucel, 2004; Liu et al., 2007; Wang et al., 2007). Hence, nonlinear analysis is necessitated for the whirling rotor under external excitation. Nonlinear motion analysis was made of the rotor, which was externally excited by electro-mechanical shakers (Antunes et al., 1996; Grunenwald et al., 1996; Moreira et al., 2000). Subsequently, the symbolic-numerical method in combination with a spectral/Galerkin approach was recently employed to obtain the nonlinear planar and orbital motions of a rotor which was subjected to external excitation by Gaussian random force (Moreira et al., 2000, 2002). More recently, Hua et al. (2005) and Cheng et al. (2006) carried out nonlinear analysis of the rotor dynamics associated with leakage air flow through a simple annular seal by using the Muzynska model (Muzynska, 1986). As for labyrinth seals which are widely used in practical situations, the geometry of the seal cannot be simplified to the annular one, while detailed concern shall be placed on serpentine geometry of the flow path resulted from the cascaded arrangement of the seal teeth. However, a literature survey shows that nonlinear analysis of the influence of the leakage flow through complex labyrinth seals on the whirling rotor was seldom reported.

In the present study, a nonlinear motion analysis of the rotating rotor under the influence of leakage air flow through a labyrinth seal was performed. The interlocking seal as shown in Fig. 1 was chosen for study. In calculations, the nonlinear aerodynamic force on the rotor surface in the coverage of the seal clearance was reduced by using the Muzynska model, while that in the coverage of the cavity volume was obtained by using the perturbation analysis. The influence of the leakage air flow through the interlocking seal on the orbital motion of the rotor was elaborated in terms of the rotating speed and inlet pressure. Stability of the whirling rotor was analyzed using the Liapunov first method.

2. Mathematical model

The orbital motion of the rotor subject to aerodynamic force by the leakage flow through the interlocking seal was thoroughly modeled. The torsional vibration of the rotor and its gyroscopic effects were neglected, whereas the transverse vibration of the rotor was carefully considered (Muzynska and Bently, 1990). Hence, as shown in Fig. 2, the

rotor–seal system was modeled as a Jeffcot rotor subject to leakage air flow through the interlocking seal. Previous nonlinear analysis (Muzynska and Bently, 1990; Hua et al., 2005; Cheng et al., 2006) simplified the complex labyrinth seal as an annular seal for ease of using the Muzynska model, in which the local axial velocity of the leakage fluid is prerequisite in calculation. However, such simplification in the seal geometry may be insufficient to include the complex influence associated with the serpentine flow path. Recall that in the labyrinth seal the leakage fluid flow is consecutively stagnated in the cavity volumes, which is indicative of difficulties in adapting the Muzynska model to detailed consideration. In the present study, the Muzynska model and the perturbation analysis was adopted for separately determining the nonlinear aerodynamic force on the rotor surface in the axial coverage of the seal clearances (zone I in Fig. 1) and of the cavity volumes (zone II in Fig. 1), respectively.

2.1. Calculation of the leakage air flow

The geometry of the interlocking seal with cascaded arrangement of the seal teeth on the stator and the rotor is illustrated in Fig. 1. Detailed information regarding its dimension can be found in Table 1. When the concentric rotor

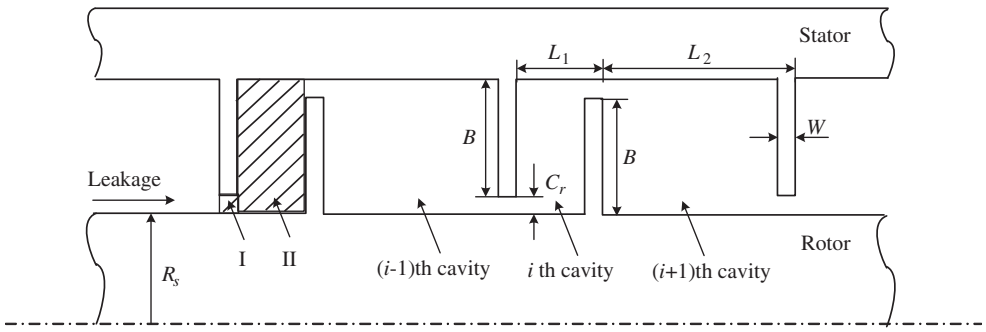

Fig. 1. Schematic diagram of the interlocking seal.

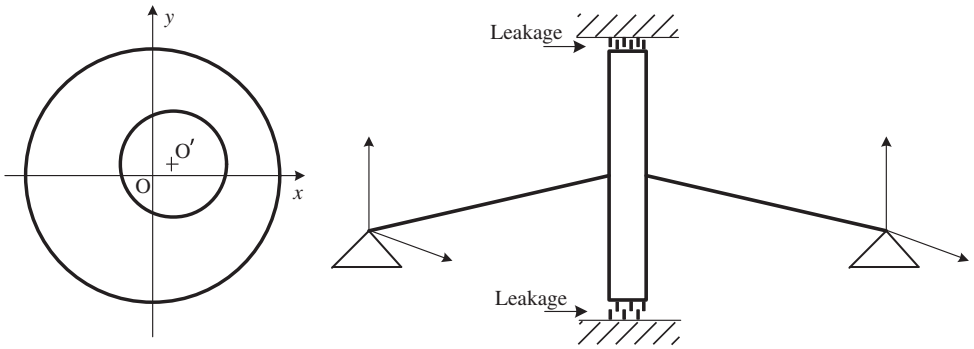

Fig. 2. Illustration of Jeffcot rotor system subject to leakage flow through the interlocking seal.

Table 1
Dimension of the interlocking seal (mm)

L_1	3	B	2.3
L_2	7	C_r	0.7
W	0.3	R_s	50

rotates at a constant speed, and the air flow through the labyrinth seal is steady and axisymmetric. Thus, the continuity equation implies that the mass flow m_i through the orifice between the seal tooth and the rotor is constant as i varies from 1 to N (Dursun and Kazakia, 1995; Dursun, 2002; Yucel, 2004):

$$m_1 = m_2 = \cdots = m_i = \cdots = m_N = m_0 = C_0 C_1 A_0 \sqrt{\frac{P_{0i-1}^2 - P_{0i}^2}{RT}}, \tag{1}$$

where m_0 is the steady-state leakage flow rate. This is employed to calculate the distribution of steady pressure P_{0i} in the cavities and the leakage flow rate m_0. The kinetic energy carry-over coefficient C_1 is equal to 1 for the first tooth, while its estimation for other teeth is given by

$$C_1 = \sqrt{\frac{N}{(1-J)N + J}}, \quad \text{with} \quad J = 1 - \frac{1}{\left(1 + 16.6\dfrac{C_r}{L}\right)^2}. \tag{2}$$

This was proposed to correct the nonuniformity of velocity distribution (Dursun and Kazakia, 1995; Yucel and Kazakia, 2001; Dursun, 2002; Yucel, 2004). The orifice contraction coefficient C_0 adopted in Eq. (1) was determined by the Chaplygin formula (Gurevich, 1966)

$$C_0 = \frac{\pi}{\pi + 2 - 5S_i + 2S_i^2}, \quad \text{with} \quad S_i = \left(\frac{P_{0i-1}}{P_{0i}}\right)^{\gamma-1/\gamma} - 1, \tag{3}$$

where γ is 1.17 for air.

When the critical condition appears at the last seal clearance, prediction of leakage air flow (Dursun and Kazakia, 1995) is determined by

$$m_0 = C_0 C_1 P_{0N-1} \frac{A_0}{\sqrt{\gamma RT}} \left(\frac{2}{\gamma + 1}\right)^{(\gamma/\gamma-1)}. \tag{4}$$

In order to solve the above system of equations, an iterative procedure is employed to calculate the leakage flow rate m_{0i} and pressure distribution P_{0i} in each seal cavity. Furthermore, the pressure at the ith tooth clearance is averaged by the pressures in the two adjacent cavities

$$P_{cli} = \frac{P_{0i-1} + P_{0i}}{2}. \tag{5}$$

Accordingly, the axial velocity at the clearance of the ith tooth is defined as

$$V_{acli} = \frac{m_{0i} RT}{A_0 P_{cli}}. \tag{6}$$

The steady circumferential velocity V_{0i} is governed by the momentum equation

$$m_0(V_{0i} - V_{0i-1}) = \tau_{r0i}\pi R_s \alpha_r L - \tau_{s0i}\pi R_s \alpha_s L, \tag{7}$$

in which the shear stress terms τ_{r0i} and τ_{s0i} are empirically estimated by Dursun and Kazakia (1995).

2.2. Aerodynamic force on the rotor surface in the coverage of the cavity volume

In practice, the inherent whirling motion of the rotor implies that variables of the leakage flow are actually unsteady and non-axisymmetric. In contrast to the seal clearance, deviation of the flow variables (pressure, circumferential velocity and shear stress) in the cavity volume from the steady and axisymmetric state would hold a weakly nonlinear relationship with the whirling rotor; these fluctuating variables are then dealt with by using perturbation analysis. As an example, the dependence of the circumferential velocity on the time t and the azimuthal position θ in the cavity volume (denoted as zone II in Fig. 1) is obtained by solving the partial differential continuity and circumferential momentum equations

$$\frac{\partial}{\partial t}(\rho_i A_n) + \frac{\rho_i V_i}{R_s}\frac{\partial A_n}{\partial \theta} + \frac{\rho_i A_n}{R_s}\frac{\partial V_i}{\partial \theta} + \frac{V_i A_n}{R_s}\frac{\partial \rho_i}{\partial \theta} + \dot{q}_{i+1} - \dot{q}_i = 0, \tag{8}$$

$$\rho_i A_n \frac{\partial V_i}{\partial t} + \frac{\rho_i V_i A_n}{R_s}\frac{\partial V_i}{\partial \theta} + (V_i - V_{i-1})\dot{q}_i = -\frac{A_n}{R_s}\frac{\partial P_i}{\partial \theta} + (\tau_{ri} a_r - \tau_{si} a_s)L, \tag{9}$$

which are further linearized using perturbation analysis. The perturbation parameter is defined as $\varepsilon = e/(C_r + B)$ for the cavity volume II as shown in Fig. 1, where e is a displacement of the rotor from the central position. Thus, the variation of the radial clearance, which is caused by the whirling motion of the rotor, is expanded in the form

$$H = C_r + \varepsilon H_1(t,\theta) + \cdots. \tag{10}$$

Correspondingly, the flow variables are expanded as

$$\begin{aligned} &P_i = P_{0i} + \varepsilon P_{1i}(t,\theta) + \cdots, \quad V_i = V_{0i} + \varepsilon V_{1i}(t,\theta) + \cdots, \quad \dot{q}_i = \dot{q}_{0i} + \varepsilon \dot{q}_{1i}(t,\theta) + \cdots, \\ &\tau_{ri} = \tau_{r0i} + \varepsilon \tau_{r1i}(t,\theta) + \cdots, \quad \tau_{si} = \tau_{s0i} + \varepsilon \tau_{s1i}(t,\theta) + \cdots. \end{aligned} \tag{11}$$

Hence, substituting these variables into Eqs. (8) and (9) and neglecting the terms of order ε^2 and higher, the first-order continuity equation for the ith cavity is reduced to

$$G_{10}\left(\frac{\partial P_{1i}}{\partial t} + \frac{V_{0i}}{R_s}\frac{\partial P_{1i}}{\partial \theta} + \frac{P_{0i}}{R_s}\frac{\partial V_{1i}}{\partial \theta}\right) + G_{20i}P_{1i-1} + G_{30i}P_{1i} + G_{40i}P_{1i+1} = -G_{50i}\left(\frac{\partial H_1}{\partial t} + \frac{V_{0i}}{R_s}\frac{\partial H_1}{\partial \theta}\right), \tag{12}$$

$$X_{10i}\left(\frac{\partial V_{1i}}{\partial t} + \frac{V_{0i}}{R_s}\frac{\partial V_{1i}}{\partial \theta}\right) + \frac{A_0}{R_s}\frac{\partial P_{1i}}{\partial \theta} + X_{20i}V_{1i} - q_0 V_{1i-1} + X_{30i}P_{1i-1} + X_{40i}P_{1i} = X_{50i}H_1, \tag{13}$$

where the terms G_{10i}, G_{20i}, G_{30i}, G_{40i}, G_{50i}, X_{10}, X_{20i}, X_{30i}, X_{40i} and X_{50i} are functions of steady pressure and velocity in the ith cavity; detailed definition of these terms can be found in Liu et al. (2007). The solution for nonlinear aerodynamic force on the rotor surface in the coverage of the cavity volume is subsequently drawn out.

The position of the rotor center at the time t is $(x_{o'}(t), y_{o'}(t))$ shown in Fig. 3. Thus, the spatio-temporal size of the seal clearance is defined as

$$H(t,\theta) = R_s + C_r - \overline{OA}, \tag{14}$$

in which

$$\overline{OA} = R_s - \varepsilon H_1(t,\theta). \tag{15}$$

The position (x_A, y_A) of the point A on the surface of the rotor is determined as

$$x_A = \overline{OA}\cos\theta, \quad y_A = \overline{OA}\sin\theta, \tag{16}$$

$$(x_A - x_{o'}(t))^2 + (y_A - y_{o'}(t))^2 = R_s^2. \tag{17}$$

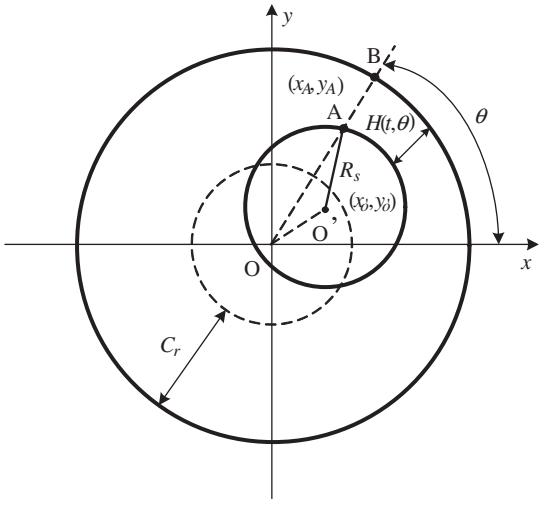

Fig. 3. Illustration of the orbital motion of the rotor.

Substituting Eqs. (15) and (16) into Eq. (17) yields the following formula:

$$H_1(t,\theta) = -\frac{2x_{o'}(t)R_s\cos\theta + 2y_{o'}(t)R_s\sin\theta - x_{o'}^2(t) - y_{o'}^2(t)}{2\varepsilon R_s - 2\varepsilon x_{o'}(t) - 2\varepsilon y_{o'}(t)}. \tag{18}$$

Under the assumption that $x_{o'}(t), y_{o'}(t) \ll R_s$, Eq. (18) can be reduced to

$$H_1(t,\theta) = -\frac{x_{o'}(t)\cos\theta + y_{o'}(t)\sin\theta}{\varepsilon}, \tag{19}$$

where

$$\varepsilon = \frac{\sqrt{x_{o'}^2(t) + y_{o'}^2(t)}}{C_r + B}. \tag{20}$$

Substituting Eq. (20) into Eq. (19) results in

$$H_1(t,\theta) = -(C_r + B)\left(\frac{x_{o'}(t)}{\sqrt{x_{o'}(t)^2 + y_{o'}(t)^2}}\cos\theta + \frac{y_{o'}(t)}{\sqrt{x_{o'}(t)^2 + y_{o'}(t)^2}}\sin\theta\right). \tag{21}$$

Eq. (21) is then rewritten as

$$H_1(t,\theta) = -(C_r + B)\mathrm{Re}\{e^{\eta(\theta-\beta)}\}, \tag{22}$$

in which $\beta = \arctan(y_{o'}(t)/x_{o'}(t))$.

Substituting Eq. (22) into Eqs. (12) and (13), we look for the solution in the following form

$$P_{1i}(t,\theta) = \mathrm{Re}\left\{P_i^+ e^{\eta(\theta+\beta)} + P_i^- e^{\eta(\theta-\beta)}\right\}, \quad V_{1i}(t,\theta) = \mathrm{Re}\left\{V_i^+ e^{\eta(\theta-\beta)} + V_i^- e^{\eta(\theta-\beta)}\right\}, \tag{23}$$

where $P_i{}^+$, $P_i{}^-$, $V_i{}^+$ and $V_i{}^-$ are constant complex coefficients ($P_i^+ = p_i^+ + \eta p'^+_i$, $P_i^- = p_i^- + \eta p'^-_i$, $V_i^+ = v_i^+ + \eta v'^+_i$, $V_i^- = v_i^- + \eta v'^-_i$). Substituting Eqs. (22) and (23) into Eqs. (12) and (13) and eliminating the terms of $e^{\eta(\theta+\beta)}$ and $e^{\eta(\theta-\beta)}$ yields a set of four linearized equations for each cavity, which are all independent of t and θ. The associated 12 unknowns included in these equations are $P_i{}^+$, $P_i{}^-$, $V_i{}^+$ and $V_i{}^-$ and their counterparts before and behind the ith cavity. The set of four equations is rearranged in the matrix form

$$\left[M_i^{-1}\right]\{Y_{i-1}\} + \left[M_i^0\right]\{Y_i\} + \left[M_i^{+1}\right]\left\{Y_{i+1}\right\} = \{E_i\}, \tag{24}$$

where

$$\{Y_i\} = \left[P_i^+, P_i^-, V_i^+, V_i^-\right]^{\mathrm{T}}, \quad \{E_i\} = \left[0, -\eta G_{50i}(C_r + B)\left(\frac{\mathrm{d}\beta}{\mathrm{d}t} - \frac{V_{0i}}{R_s}\right), 0, -X_{50i}(C_r + B)\right]^{\mathrm{T}},$$

$$\left[M_i^{-1}\right] = \begin{bmatrix} G_{20i} & 0 & 0 & 0 \\ 0 & G_{20i} & 0 & 0 \\ X_{30i} & 0 & -q_0 & 0 \\ 0 & X_{30i} & 0 & -q_0 \end{bmatrix},$$

$$\left[M_i^0\right] = \begin{bmatrix} \eta G_{10}\left(\frac{V_{0i}}{R_s} + \frac{\mathrm{d}\beta}{\mathrm{d}t}\right) + G_{30i} & 0 & \eta G_{10}\frac{P_{0i}}{R_s} & 0 \\ 0 & \eta G_{10}\left(\frac{V_{0i}}{R_s} - \frac{\mathrm{d}\beta}{\mathrm{d}t}\right) + G_{30i} & 0 & \eta G_{10}\frac{P_{0i}}{R_s} \\ \eta\frac{A_0}{R_s} + X_{40i} & 0 & \eta X_{10i}\left(\frac{V_{0i}}{R_s} + \frac{\mathrm{d}\beta}{\mathrm{d}t}\right) + X_{20i} & 0 \\ 0 & \eta\frac{A_0}{R_s} + X_{40i} & 0 & \eta X_{10i}\left(\frac{V_{0i}}{R_s} - \frac{\mathrm{d}\beta}{\mathrm{d}t}\right) + X_{20i} \end{bmatrix},$$

$$\left[M_i^{+1}\right] = \begin{bmatrix} G_{40i} & 0 & 0 & 0 \\ 0 & G_{40i} & 0 & 0 \\ 0 & 0 & 0 & 0 \\ 0 & 0 & 0 & 0 \end{bmatrix}.$$

Here, the shaking frequency $\mathrm{d}\beta/\mathrm{d}t$ is defined as

$$\frac{\mathrm{d}\beta}{\mathrm{d}t} = \frac{[y_{o'}(t)]' x_{o'}(t) - [x_{o'}(t)]' y_{o'}(t)}{x_{o'}(t)^2},$$

which was simultaneously obtained by iterative calculation of the orbit of the whirling rotor.

Close inspection of Eq. (23) shows that the four linearized equations are associated with each cavity. For a labyrinth seal with N cavities, this results in a $4(N-1)\times 4(N-1)$ banded system of the linear Eq. (24) which determines the $4(N-1)$ unknowns P_i^+, P_i^-, V_i^+ and V_i^- for $i = 1, 2, \cdots, N-1$,

$$\begin{bmatrix} M_0^0 & M_0^{+1} & & & & & & & & & & \\ M_1^{-1} & M_1^0 & M_1^{+1} & & & & & & & & & \\ \bullet & \bullet & \bullet & & & & & & & & & \\ & & & M_{i-1}^{-1} & M_{i-1}^0 & M_{i1-}^{+1} & & & & & & \\ & & & & M_i^{-1} & M_i^0 & M_i^{+1} & & & & & \\ & & & & & M_{i+1}^{-1} & M_{i+1}^0 & M_{i+1}^1 & & & & \\ & & & & & & & & \bullet & \bullet & \bullet & \\ & & & & & & & & M_{N-2}^{-1} & M_{N-2}^0 & M_{N-2}^{+1} & \\ & & & & & & & & & M_{N-1}^0 & M_{N-1}^{+1} & \end{bmatrix} \begin{bmatrix} Y_0 \\ Y_1 \\ \bullet \\ Y_{i-1} \\ Y_i \\ Y_{i+1} \\ \bullet \\ Y_{N-2} \\ Y_{N-1} \end{bmatrix} = \begin{bmatrix} E_0 \\ E_1 \\ \bullet \\ E_{i-1} \\ E_i \\ E_{i+1} \\ \bullet \\ E_{N-2} \\ E_{N-1} \end{bmatrix}. \tag{25}$$

Hence, the set of Eq. (25) is readily solved by using Gauss elimination method.

The total net force F which is acted on the rotor surface in the coverage of the cavity volumes can be obtained by integrating the disturbance pressure and disturbance shear stress along the rotor surface

$$F(t)\big|_{ca} = F_x + \eta F_y = -\varepsilon R_s L \sum_{i=1}^{N-1} \int_0^{2\pi} (P_{1i} \mathrm{e}^{\eta\theta} - \eta\alpha_r \tau_{r1i} \mathrm{e}^{\eta\theta})\, \mathrm{d}\theta, \tag{26a}$$

$$\begin{aligned} F(t)\big|_{ca} = & -\varepsilon\pi R_s L \sum_{i=1}^{N-1} \left\{ \overline{P_i^-}\left(1 - \eta\alpha_r \frac{\tau_{r0i}}{P_{0i}}\right) - \eta\alpha_r \left[\frac{1.75\tau_{r0i}}{V_{0i} - R_s\omega}\overline{V_i^-} + \frac{0.125\tau_{r0i} Dh_0}{(B + C_r)^2}(C_r + B)\right] \right\} \mathrm{e}^{\eta\beta} \\ & + \left\{ \overline{P_i^+}\left(1 - \eta\alpha_r \frac{\tau_{r0i}}{P_{0i}}\right) - \eta\alpha_r \frac{1.75\tau_{r0i}}{V_{0i} - R_s\omega}\overline{V_i^+} \right\} \mathrm{e}^{-\eta\beta}; \end{aligned} \tag{26b}$$

then the cavity reaction force components are given as

$$\begin{cases} F_x(t)\big|_{ca} = -\varepsilon R_s L \sum\limits_{i=1}^{N-1} \left\{ \left(Coef_1 + Coef_2\right)\cos\beta + \left(Coef_3 - Coef_4\right)\sin\beta \right\}, \\ F_y(t)\big|_{ca} = -\varepsilon R_s L \sum\limits_{i=1}^{N-1} \left\{ \left(Coef_1 - Coef_2\right)\sin\beta - \left(Coef_3 + Coef_4\right)\cos\beta \right\}, \end{cases} \tag{27}$$

where

$$\begin{cases} Coef_1 = p_i^- - p'^-_i \alpha_r \dfrac{\tau_{r0i}}{P_{0i}} - v'^-_i \alpha_r \dfrac{1.75\tau_{r0i}}{V_{0i} - \omega R_s}, \quad Coef_2 = p_i^+ - p'^+_i \alpha_r \dfrac{\tau_{r0i}}{P_{0i}} - v'^-_i \alpha_r \dfrac{1.75\tau_{r0i}}{V_{0i} - \omega R_s}, \\ Coef_3 = p_i^- \alpha_r \dfrac{\tau_{r0i}}{P_{0i}} + p'^-_i + v_i^- \alpha_r \dfrac{1.75\tau_{r0i}}{V_{0i} - \omega R_s} + \alpha_r \dfrac{0.125\tau_{r0i} Dh_0}{(B + C_r)^2}(C_r + B), \quad Coef_4 = p_i^+ \alpha_r \dfrac{\tau_{r0i}}{P_{0i}} + p'^+_i + v_i^+ \alpha_r \dfrac{1.75\tau_{r0i}}{V_{0i} - \omega R_s}. \end{cases} \tag{28}$$

2.3. Aerodynamic force on the rotor surface in the coverage of the seal clearance

The aforementioned calculation of the aerodynamic force on the rotor surface in the coverage of the cavity volume is performed by using the perturbation analysis. The perturbation analysis is well suited for linear or weakly nonlinear behaviors under the condition that the local eccentricity ratio (ε) of the disturbed rotor is far less than 1.0; here, the term ε is determined to be $e/(C_r+B)$ and e/C_r for the cavity volume and the seal clearance, respectively. The fact C_r is usually far less than B indicates that Eq. (27) based on the perturbation analysis cannot be readily used for the case of the leakage flow through the seal clearance, where the local aerodynamic force on the rotor surface may be strongly coupled with the whirling rotor. Hereafter, we turn to the Muzynska, (1986) model for an accurate derivation of the aerodynamic force on the rotor surface in the coverage of the seal clearance which is denoted as zone I in Fig. 1.

By using the Muzynska model, the aerodynamic force on the rotor surface in the coverage of the seal clearance is formulated as

$$\left\{\begin{matrix} F_x \\ F_y \end{matrix}\right\}\Bigg|_{cl} = -\begin{bmatrix} K-\tau^2\omega^2 m_f & \tau\omega D \\ -\tau\omega D & K-\tau^2\omega^2 m_f \end{bmatrix}\left\{\begin{matrix} X \\ Y \end{matrix}\right\} - \begin{bmatrix} D & 2\tau\omega m_f \\ -2\tau\omega m_f & D \end{bmatrix}\left\{\begin{matrix} \dot{X} \\ \dot{Y} \end{matrix}\right\} - \begin{bmatrix} m_f & 0 \\ 0 & m_f \end{bmatrix}\left\{\begin{matrix} \ddot{X} \\ \ddot{Y} \end{matrix}\right\}, \tag{29}$$

where τ is the ratio of the averaged circumferential velocity of the local leakage fluid to rotating speed ω of the rotor [τ is approximated to 0.5 (Muzynska and Bently, 1990)], F_x and F_y are the local aerodynamic forces in the X and Y coordinates, respectively. In Eq. (29), K, D and m_f are equivalent stiffness, equivalent damping and equivalent mass, respectively; these are all nonlinear functions of the radial displacement $(x_{o'}(t), y_{o'}(t))$ of the rotor (Muzynska and Bently, 1990)

$$\begin{aligned} &K = K_0(1-\varepsilon^2)^{-nn}, \quad D = D_0(1-\varepsilon^2)^{-nn}, \quad nn = \frac{1}{2}\sim 3, \\ &\tau = \tau_0(1-\varepsilon)^b, \quad 0<b<1, \quad m_f = \mu_2\mu_3 t_{cl}^2, \end{aligned} \tag{30}$$

where the empirical parameter nn is set to 2 (Li and Xu, 2003). In Eq. (30), the eccentricity ratio ε is defined as

$$\varepsilon = \frac{\sqrt{x_{o'}^2(t)+y_{o'}^2(t)}}{C_r}. \tag{31}$$

Furthermore, K_0 and D_0 in Eq. (30) are given by Childs (1983)

$$K_0 = \mu_0\mu_3, \quad D_0 = \mu_1\mu_3 t_{cl}, \tag{32}$$

where

$$\begin{aligned} &\mu_0 = \frac{2\sigma^2}{1+z+2\sigma}E(1-g_0), \quad \mu_1 = \frac{2\sigma^2}{1+z+2\sigma}\left[\frac{E}{\sigma}+\frac{U}{2}\left(\frac{1}{6}+E\right)\right], \quad \mu_2 = \frac{\sigma(1/6+E)}{1+z+2\sigma}, \\ &\mu_3 = \frac{\pi R_s(P_{0i-1}-P_{0i})}{\lambda}, \quad t_{cl} = \frac{W}{V_{acli}}, \end{aligned} \tag{33}$$

and

$$\begin{aligned} &\lambda = n_0 R_a^{g_0}\left[1+\left(\frac{R_v}{R_a}\right)^2\right]^{(1+g_0/2)}, \quad \sigma = \frac{\lambda W}{C_r}, \quad E = \frac{1+z}{1+z+2\sigma}, \quad U = 2-\frac{(R_v/R_a)^2-g_0}{(R_v/R_a)^2+1}, \\ &R_v = \frac{R_s C_r \omega}{v}, \quad R_a = \frac{2V_{acli}C_r}{v}. \end{aligned} \tag{34}$$

Here, the parameters are determined to $z=0.1$, $n_0=0.079$, $g_0=-0.25$ (Li and Xu, 2003). Note that the local axial velocity of the leakage flow is required for calculation of t_{cl} and R_a.

For a labyrinth seal with N teeth, the total aerodynamic force on the rotor surface in the coverage of the seal clearances can be obtained by integrating the associated forces

$$\left\{\begin{matrix} F_x(t) \\ F_y(t) \end{matrix}\right\}\Big|_{cl} = \left\{\begin{matrix} \sum_{i=1}^{N-1} F_{xi} \\ \sum_{i=1}^{N-1} F_{yi} \end{matrix}\right\} = - \begin{bmatrix} \sum_{i=1}^{N}\left(K_i - \tau_i^2\omega^2 m_{fi}\right) & \sum_{i=1}^{N}\tau_i\omega D_i \\ -\sum_{i=1}^{N}\tau_i\omega D_i & \sum_{i=1}^{N}\left(K_i - \tau_i^2\omega^2 m_{fi}\right) \end{bmatrix} \left\{\begin{matrix} X \\ Y \end{matrix}\right\} - \begin{bmatrix} \sum_{i=1}^{N} D_i & 2\sum_{i=1}^{N}\tau_i\omega m_{fi} \\ -2\sum_{i=1}^{N}\tau_i\omega m_{fi} & \sum_{i=1}^{N} D_i \end{bmatrix} \left\{\begin{matrix} \dot{X} \\ \dot{Y} \end{matrix}\right\} - \begin{bmatrix} \sum_{i=1}^{N} m_{fi} & 0 \\ 0 & \sum_{i=1}^{N} m_{fi} \end{bmatrix} \left\{\begin{matrix} \ddot{X} \\ \ddot{Y} \end{matrix}\right\}. \tag{35}$$

2.4. Governing equation of rotor dynamics

The stabilization and response of the rotor system subject to aerodynamic forces induced by leakage air flow through the labyrinth seal is characterized by the governing equation of rotor dynamics

$$\begin{bmatrix} m_r & 0 \\ 0 & m_r \end{bmatrix} \left\{\begin{matrix} \ddot{X} \\ \ddot{Y} \end{matrix}\right\} + \begin{bmatrix} D_e & 0 \\ 0 & D_e \end{bmatrix} \left\{\begin{matrix} \dot{X} \\ \dot{Y} \end{matrix}\right\} + \begin{bmatrix} K_e & 0 \\ 0 & K_e \end{bmatrix} \left\{\begin{matrix} X \\ Y \end{matrix}\right\} = \left\{\begin{matrix} F_x \\ F_y \end{matrix}\right\}\Big|_{cl} + \left\{\begin{matrix} F_x \\ F_y \end{matrix}\right\}\Big|_{ca} + \left\{\begin{matrix} F_x \\ F_y \end{matrix}\right\}_{br} - \left\{\begin{matrix} 0 \\ m_r g \end{matrix}\right\}, \tag{36}$$

in which the dimensionless parameters are defined as

$$x = X/C_r, \quad y = Y/C_r, \quad \omega t_{cl} = \bar{T}, \quad M = m_r + \sum m_f + \sum m_{fbr},$$
$$\dot{X} = \dot{x}\omega C_r, \quad \ddot{X} = \dot{x}\omega^2 C_r, \quad \dot{Y} = \dot{y}\omega C_r, \quad \ddot{Y} = \ddot{y}\omega^2 C_r. \tag{37}$$

It is of note that in the present study the nonlinear oil film forces $F_x|_{br}$ and $F_y|_{br}$ exerted by the annular journal bearings are also calculated by using the Muzynska model presented in Section 2.3.

Substituting Eq. (37) into Eq. (36) and leaving the total aerodynamic force to the left hand of the equation leads to the following set of governing equations

$$\begin{bmatrix} 1 & 0 \\ 0 & 1 \end{bmatrix} \left\{\begin{matrix} \ddot{x} \\ \ddot{y} \end{matrix}\right\} + \begin{bmatrix} D_1 & D_2 \\ -D_2 & D_1 \end{bmatrix} \left\{\begin{matrix} \dot{x} \\ \dot{y} \end{matrix}\right\} + \begin{bmatrix} K_1 & K_2 \\ -K_2 & K_1 \end{bmatrix} \left\{\begin{matrix} x \\ y \end{matrix}\right\} = \left\{\begin{matrix} G_1 \\ G_2 \end{matrix}\right\}, \tag{38}$$

where

$$K_1 = \frac{K_e + (K_{br} - \tau_{br}^2\omega^2 m_{fbr}) + \sum_{i=1}^{N}(K_i - \tau_i^2\omega^2 m_{fi})}{M\omega^2}, \quad K_2 = \frac{\tau_{br}D_{br} + \sum_{i=1}^{N}\tau_i D_i}{M\omega},$$
$$D_1 = \frac{D_e + D_{br} + \sum_{i=1}^{N} D_i}{M\omega}, \quad D_2 = \frac{2\tau_{br}D_{br} + 2\sum_{i=1}^{N}\tau_i D_i}{M}, \quad G_1 = \frac{F_x(t)\big|_{ca}}{MC_r\omega^2}, \quad G_2 = \frac{F_y(t)\big|_{ca} - m_r g}{MC_r\omega^2}. \tag{39}$$

In the calculations, Eq. (38) is solved by using the fourth-order Runge–Kutta method to obtain the orbit of the whirling rotor.

2.5. Stability analysis

Stability analysis of the whirling rotor, which is under the influence of leakage air flow through the interlocking seal, is subsequently carried out by using the Liapunov first method. Toward this end, Eq. (38) is

rearranged as

$$\begin{Bmatrix} \ddot{x} \\ \ddot{y} \\ \dot{x} \\ \dot{y} \end{Bmatrix} + \begin{bmatrix} -D_1 & -D_2 & -K_1 & -K_2 \\ D_2 & -D_1 & K_2 & -K_1 \\ 1 & 0 & 0 & 0 \\ 0 & 1 & 0 & 0 \end{bmatrix} \begin{Bmatrix} \dot{x} \\ \dot{y} \\ x \\ y \end{Bmatrix} + \begin{Bmatrix} G_1 \\ G_2 \\ 0 \\ 0 \end{Bmatrix} = \begin{Bmatrix} f_1(\dot{x}, \dot{y}, x, y, \omega) \\ f_2(\dot{x}, \dot{y}, x, y, \omega) \\ f_3(\dot{x}, \dot{y}, x, y, \omega) \\ f_4(\dot{x}, \dot{y}, x, y, \omega) \end{Bmatrix}. \tag{40}$$

The stability of the rotor–seal system is determined by eigenvalues of the first approximate expression of Eq. (40). Hence, approximate expansion of Eq. (40) at the balanced position (x_0, y_0) is performed to obtain a Jacobi matrix

$$J = Df\big|_{(x_0,y_0)} = \begin{bmatrix} \frac{\partial f_1}{\partial \dot{x}} & \frac{\partial f_1}{\partial \dot{y}} & \frac{\partial f_1}{\partial x} & \frac{\partial f_1}{\partial y} \\ \frac{\partial f_2}{\partial \dot{x}} & \frac{\partial f_2}{\partial \dot{y}} & \frac{\partial f_2}{\partial x} & \frac{\partial f_2}{\partial y} \\ \frac{\partial f_3}{\partial \dot{x}} & \frac{\partial f_3}{\partial \dot{y}} & \frac{\partial f_3}{\partial x} & \frac{\partial f_3}{\partial y} \\ \frac{\partial f_4}{\partial \dot{x}} & \frac{\partial f_4}{\partial \dot{y}} & \frac{\partial f_4}{\partial x} & \frac{\partial f_4}{\partial y} \end{bmatrix}, \tag{41}$$

where the balanced position (x_0, y_0) is obtained from

$$\begin{bmatrix} K_1 & K_2 \\ -K_2 & K_1 \end{bmatrix} \begin{Bmatrix} x_0 \\ y_0 \end{Bmatrix} = \begin{Bmatrix} G_1 \\ G_2 \end{Bmatrix}. \tag{42}$$

Hence, stability of the nonlinear system is assessed by inspecting the eigenvalues $a_j \pm \eta b_j$ of Eq. (41) (Zubov, 1973). The nonlinear system is stable when $a_j < 0$ ($j = 1, 2$), while the critical condition of the nonlinear system is reached when $a_j = 0$ for a pair of eigenvalues and $a_j < 0$ for the others. When $a_j > 0$ ($j = 1$ or 2) for a pair of conjugate complex numbers $a_j \pm \eta b_j$, the nonlinear system is destabilized.

3. Results and discussion

The orbital motions of the rotor at various operating conditions displayed in Table 2 were calculated in the present study. The inlet circumferential velocity V_0 was fixed to 0 (Li and Xu, 2003). For the condition $n = 3$, $N = 16$, $R_s = 50$, the orbital motions of the rotor at different rotating speeds $\omega = 3000$, 4000, 5000 and 6000 rpm are shown in Fig. 4. As shown in Fig. 4, orbits of the whirling rotor at $\omega = 3000$ and 4000 rpm are not distinctly deviated from the central position; the deviation ε is far less than 0.01 in the labyrinth seals. This means that the nonlinear characteristics between the whirling rotor and the leakage flow through the labyrinth seal are weak. However, when the rotating speed of the rotor reaches 5000 or 6000 rpm, the deviation ε of the rotor from the statically balanced position is greater than 0.1 in the coverage of the seal clearance, while ε is still less than 0.02 in the coverage of the cavity volume. This indicates the existence of the strongly nonlinear interaction between the rotating rotor and the leakage flow through the seal clearance.

Further understanding of the influence of the leakage air flow on the whirling rotor is gained through varying the pressure ratio n while the rotating speed of the rotor ($N = 16$, $R_s = 50$ mm) is fixed at $\omega = 4000$ rpm. The orbital motions of the rotor at $n = 1$, 2, 3, 4, 5 and 6 are shown in Fig. 5. Inspection of Fig. 5 demonstrates that the orbital magnitude of the whirling rotor is increased with increasing the pressure ratio, which is attributed to the intensified aerodynamic force on the rotor surface. Furthermore, the dependence of the orbital motion of the rotor on the rotating

Table 2
Operating conditions of the interlocking seal

Pressure ratio, n	1, 2, 3, 4, 5, 6
Rotating speed, ω (rpm)	3000, 4000, 5000, 6000
Inlet circumferential velocity, V_0 (m/s)	0
Tooth number, N	16, 20, 24, 26, 32, 36, 40, 44
Radius of the rotor, R_s (mm)	50, 60, 70, 80, 90, 100, 110, 120

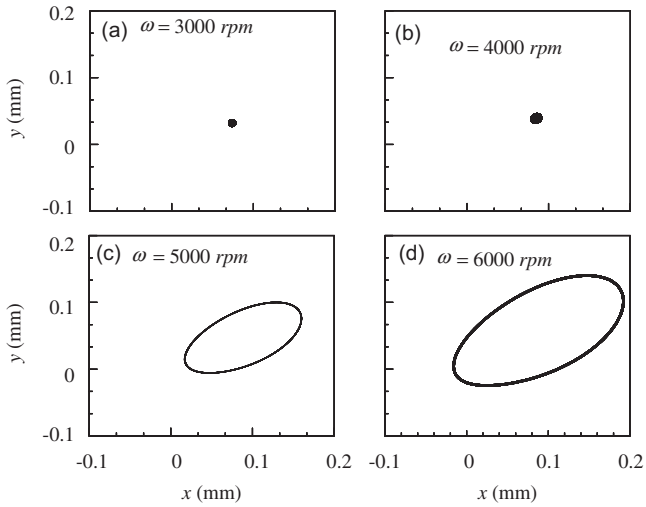

Fig. 4. The orbital motion of the rotor at different rotating speeds ($n = 3$): (a) $\omega = 3000$ rpm, (b) $\omega = 4000$ rpm, (c) $\omega = 5000$ rpm and (d) $\omega = 6000$ rpm.

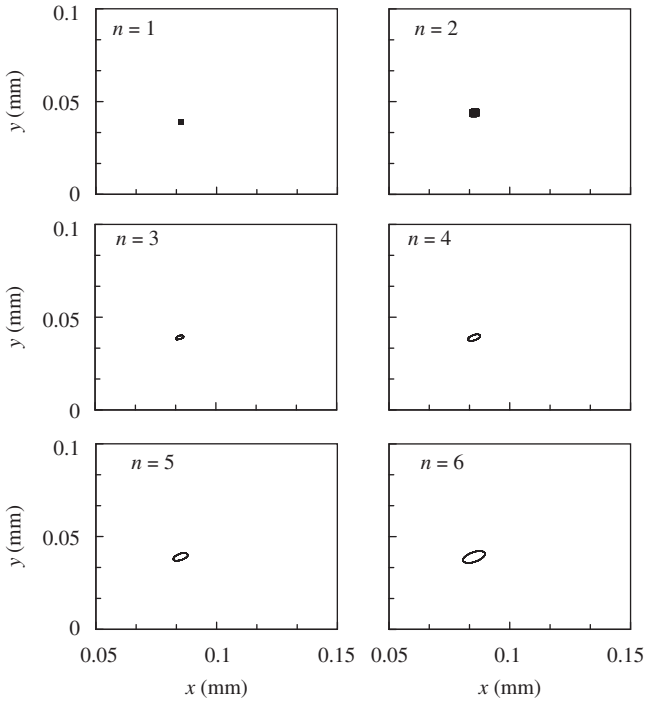

Fig. 5. The orbital motion of the rotating rotor at different pressure ratios ($\omega = 4000$ rpm).

speed is seen from Fig. 6, in which the numerical results at the conditions with and without considering the aerodynamic force ($n = 6$) are provided for detailed comparison. The orbital magnitude of the whirling rotor is increased on going from $\omega = 4000$ to 4350 rpm, indicating the destabilized influence of the rotating speed on the rotor. Comparison of the orbital motion at the conditions with and without consideration of the aerodynamic force discloses that the orbital magnitude at the former condition is larger, indicating the destabilization of the rotating rotor due to the intensified influence of the leakage flow through the interlocking seal.

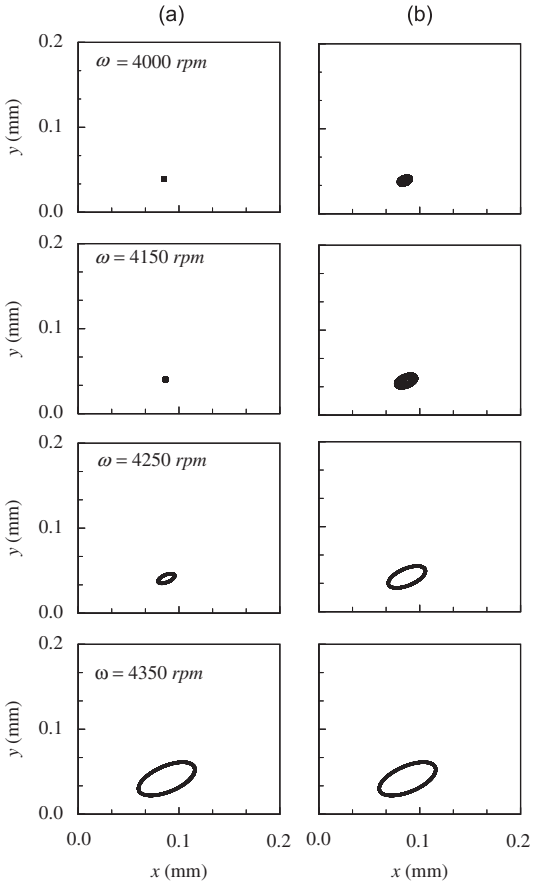

Fig. 6. The orbital motion of the rotor at different rotating speeds ($n = 6$): (a) without aerodynamic force; (b) with aerodynamic force.

Table 3
Eigenvalues of Jacobi matrix at different rotating speeds of the rotor

Rotating speed (rpm)	X_1	X_2	X_3	X_4
(a) Without aerodynamic force				
4007	$-0.39+0.47\eta$	$-0.39-0.47\eta$	$-0.01+0.50\eta$	$-0.01-0.50\eta$
4193	$-0.38+0.45\eta$	$-0.38-0.45\eta$	$0.00+0.48\eta$	$0.00-0.48\eta$
4475	$-0.35+0.43\eta$	$-0.35-0.43\eta$	$0.01+0.45\eta$	$0.01-0.45\eta$
(b) With aerodynamic force				
4002	$-0.39+0.47\eta$	$-0.39-0.47\eta$	$-0.01+0.50\eta$	$-0.01-0.50\eta$
4179	$-0.37+0.45\eta$	$-0.37-0.45\eta$	$0.00+0.48\eta$	$0.00-0.48\eta$
4460	$-0.35+0.43\eta$	$-0.35-0.43\eta$	$0.01+0.45\eta$	$0.01-0.45\eta$

Now we turn to stability analysis of the rotating rotor subject to the leakage flow. Table 3 displays the numerical results at $N = 16$, $R_s = 50$ mm by using Liapunov first method. The eigenvalues of Jacobi matrix shown in Table 3 determine that the destabilization speed of the rotor under the influence of the leakage flow is 4179 rpm, while it is increased to 4193 rpm when the influence of the leakage flow is not taken into account. This convincingly demonstrates the destabilization influence of the leakage air flow on the rotating rotor.

Geometrical influence of the rotor–seal system on stability of the rotor is obtained by varying the number of seals (N) and the radius of the rotor (R_s) while the pressure ratio is fixed to $n = 6$. Fig. 7 shows the destabilization speed of the

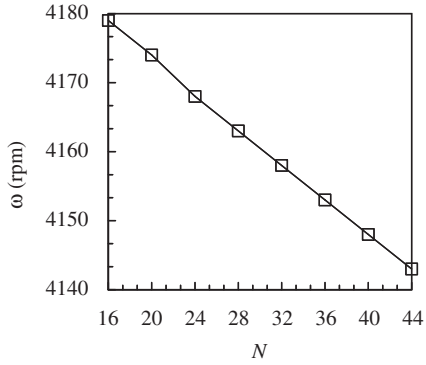

Fig. 7. Dependence of the destabilization speed on the number of teeth ($n = 6$).

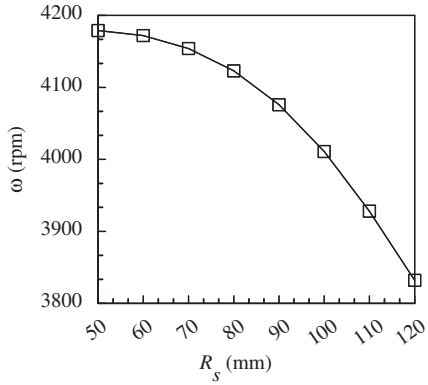

Fig. 8. Dependence of the destabilization speed on the radius of the rotating rotor ($n = 6$).

rotating rotor at various conditions with different number of seal teeth. It is clear that the destabilization speed is linearly reduced with increasing the number of the seal teeth. The dependence of the destabilization speed on the radius of the rotor is shown in Fig. 8. The destabilization speed is reduced when the radius of the rotor increases, which might be due to the enhanced aerodynamic forcing. In addition, the reduction rate of the destabilization speed is sharply intensified with increasing the radius of the rotor.

4. Conclusion

A nonlinear analysis of the influence of leakage air flow through an interlocking seal on the orbital motion of a rotor was given in the present study. The rotor–seal system was modeled as a Jeffcot rotor subject to aerodynamic force induced by the leakage flow. Particular attention was given to the serpentine flow path by spatially separating the aerodynamic force on the rotor surface into two parts, i.e., the seal clearance and the cavity volume. The aerodynamic force associated with the seal clearance, which is strongly coupled with the whirling rotor, was obtained by using the Muzynska model. The perturbation analysis was employed to delineate the spatio-temporal variation of the pressure and the shear stress on the rotor. The unsteady aerodynamic force integrated at all seal clearances and cavity volumes were incorporated into the governing equation of the rotor dynamics, which was then solved by using the fourth-order Runge–Kutta method for further nonlinear analysis. Stability of the rotating rotor was inspected by employing the Liapunov first method. The orbital motion of the rotor was analyzed in terms of the pressure ratio and the rotating speed. The orbital magnitude of the rotor with leakage flow was shown to be larger than that without leakage flow, which indicates the intensified influence of the leakage flow on stabilization of the rotating rotor. Stability analysis by

using the Liapunov first method convincingly demonstrated that the destabilization speed of the rotor was reduced due to aerodynamic force of the leakage flow.

Acknowledgement

This work was supported by grants (nos.10732060 and 50606024) from national Natural Science Foundation of China (NSFC).

References

Antunes, J., Axisa, F., Grunenwald, T., 1996. Dynamics of rotors immersed in eccentric annular flow: part 1—theory. Journal of Fluids and Structures 10, 893–918.

Cheng, M., Meng, G., Jin, J.P., 2006. Non-linear dynamics of a rotor–bearing–seal system. Archive of Applied Mechanics 76, 215–227.

Childs, D.W., 1983. Dynamic analysis of turbulent annular seals based on Hir's lubrication equation. ASME Journal of Lubrication Technology 105, 429–436.

Childs, D.W., Scharrer, J.K., 1986. An Iwatsubo-based solution for labyrinth seals: comparison to experimental results. ASME Journal of Engineering for Gas Turbines and Power 108, 325–331.

Childs, D.W., Scharrer, J.K., 1987. Theory versus experiment for the rotordynamic coefficients of labyrinth gas seals: part II—a comparison to experiment. Rotating Machinery Dynamics, vol. 2. In: Proceedings from ASME Conference on Mechanical Vibration and Noise, Boston, MA, pp. 427–434.

Dursun, E., 2002. Rotordynamic coefficients in stepped labyrinth seals. Computer Methods in Applied Mechanics and Engineering 191, 3127–3135.

Dursun, E., Kazakia, J.Y., 1995. Air flow in cavities of labyrinth seals. International Journal of Engineering Science 33, 2309–2326.

Grunenwald, T., Axisa, F., Bennett, G., 1996. Dynamics of rotors immersed in eccentric annular flow: part 2—experiments. Journal of Fluids and Structures 10, 914–944.

Gurevich, M.I., 1966. The Theory of Jets in an Ideal Fluid. Pergamon Press, Oxford, pp. 319–323.

Hua, J., Swaddiwudhipong, S., Liu, Z.S., Xu, Q.Y., 2005. Numerical analysis of nonlinear rotor–seal system. Journal of Sound and Vibration 283, 525–542.

Iwatsubo, T., 1980. Evaluation of instability forces of labyrinth seals in turbines or compressors. In: Rotordynamic Instability Problems in High-Perfomance Turbomachinery. NASA CP, 2133, pp. 139–167.

Kleynhans, G., 1996. A two-control-volume bulk-flow rotordynamic analysis for smooth-rotor/honeycomb-stator gas annular seal. Dissertation, Mechanical Engineering, Texas A&M University, pp. 55–57.

Kostyuk, A.G., 1972. A theoretical analysis of the aerodynamic forces in the labyrinth glands of turbomachines. Teploenergetica 19, 29–33.

Li, S.T., Xu, Q.Y., 2003. Stability and bifurcation of unbalance rotor/labyrinth seal system. Applied Mathematics and Mechanics 24, 1290–1301.

Liu, Y.Z., Wang, W.Z., Chen, H.P., Ge, Q., Yuan, Y., 2007. Influence of leakage flow through labyrinth seals on rotordynamics: numerical calculations and experimental measurements. Archive of Applied Mechanics 77, 601–603.

Moreira, M., Antunes, J., Pina, H., 2000. A theoretical model for nonlinear orbital motions of rotors under fluid confinement. Journal of Fluids and Structures 14, 635–668.

Moreira, M., Antunes, J., Pina, H., 2002. Nonlinear analysis of the orbital motions of immersed rotors using a spectral/Galerkin approach. Communications in Nonlinear Science and Numerical Simulation 7, 123–137.

Muzynska, A., 1986. Whirl and whip-rotor/bearing stability problems. Journal of Sound and Vibration 110, 443–462.

Muzynska, A., Bently, D.E., 1990. Frequency-swept rotating input perturbation techniques and identification of the fluid force models in rotor/bearing/seal systems and fluid handling machines. Journal of Sound and Vibration 143, 103–124.

Rosen, M.C., 1986. University of Virginia Report ♯UVA/643092/MAE86/346.

Wang, W.Z., Liu, Y.Z., Chen, H.P., Jiang, P.N., 2007. Computation of rotordynamic coefficients associated with leakage steam flow through labyrinth seal. Archive of Applied Mechanics 77, 589–595.

Yucel, U., Kazakia, J.Y., 2001. Analytical prediction techniques for axisymmetric flow in gas labyrinth seals. ASME Journal of Engineering for Gas Turbines and Power 123, 255–257.

Yucel, U., 2004. Calculation of leakage and dynamic coefficients of stepped labyrinth gas seals. Applied Mathematics and Computation 152, 521–533.

Zubov, V.I., 1973. Stability of Motion: Liapunov Methods and Their Application. Izdatel'stvo Vysshaia Shkola, Moscow.